https://erjm.journals.ekb.eg
ISSN: 1110-1180
DOI: ---------

ERJ
Engineering Research Journal
Faculty of Engineering
Menoufia University

# Numerical Investigation on Torsional Reinforced Concrete Stepped Beams with Various Reinforcement Patterns

**Boshra A. Eltaly [1], Ahmed F. Elkhouly [1*], Fathi A. Abdelmgeed [2], Ahmed Khalifa [2,3]**

[1] *Civil Engineering Dept., Faculty of Engineering, Menoufia University, Egypt*
[2] *Civil Engineering Dept., Faculty of Engineering Kafr Elshiekh University, Egypt*
[3] *M. Sc. Candidate, Civil Engineering Dept., Faculty of Engineering Menoufia University, Egypt*
**(Corresponding author: Ahmed.elkholy@sh-eng.menofia.edu.eg)*

**ABSTRACT**
A Finite Element Model (FEM) for Reinforcement Concrete Stepped Beams (RCSBs) is presented in this numerical investigation, aiming to capture the effect of Stirrups Spacings (SSs), Stirrups' Diameters (SDs), Longitudinal Reinforcement Ratio (LRR), and Longitudinal Reinforcement Patterns (LRP) as a various parameters effect on the structural performance of RCSBs under pure torsion loads. Implemented using ABAQUS and validated against previous experimental results, the study included a parametric analysis of 10 beams divided into 4 groups, focusing on the distance of SSs with varied lengths, SDs with varied diameter and configurations, more ratios of LRR, and different LRP of longitudinal bars. To compare the beams, both elastic stiffness (K) and ductility (D) and absorbed energy (E) were calculated. Straight beams exhibit superior torsional properties than the (RCSBs). The results indicated that changing in (LRR), (SDs), (LRP), (SSs) led to a decrease in the torsional moment capacity by 3-5%, 9-13%, 26-32%, 17-36%, respectively of their values to beam B0. In addition to enhancing the elastic and ductile stiffness as well as the absorbed energy of each specimen.

***Keywords:*** *Reinforced concrete stepped beam; Stirrups spacings; Stirrups' diameters; Longitudinal reinforcement ratio; Longitudinal reinforcement patterns.*

## 1. Introduction

In structural engineering, elements subjected to torsional loads are extremely important since they are essential to the stability and operation of many different types of structures, such as towers, bridges, and buildings. Twisting effects produced by torsional loads can significantly alter the distribution of stresses and patterns of deformation in structural materials, possibly leading to failure modes that are different from those brought on by shear or bending forces. To preserve structural integrity and safety, these loads must be understood and mitigated properly. Research has shown that inadequate torsional impact design can lead to serious failures including concrete cover spalling and diagonal cracking, endangering the overall performance of the structure [1-6].

Numerous techniques exist for strengthening reinforced concrete (RC) beams subjected to torsional forces; these techniques use various materials to increase torsional capacity, stiffness, and overall structural performance. Using externally bonded fiber-reinforced polymer (FRP) composites, such as glass fiber-reinforced polymer (GFRP) [7-11] or carbon fiber-reinforced polymer (CFRP) [12-14], is one efficient technique. When used as sheets or wraps, these composites offer excellent tensile strength and longevity, which improves the beams' torsional capacity and ductility. Moreover, techniques like steel plate bonding [15, 16], which involves attaching steel plates using epoxy adhesives, and concrete jacketing, which adds additional layers of concrete in addition to steel reinforcement, give the beams more strength and stiffness.

Geometric elements such as openings can greatly affect the torsional behavior of RC girders, often diminishing their ability to withstand torsional forces. To counteract this, several reinforcement techniques are used to boost torsional performance. One effective method involves using fiber-reinforced polymer (FRP) composites, including carbon or glass fibers, which significantly improve both torsional stiffness and strength. According to research by Eltaly et al [17], the use of FRP composites, like CFRP and GFRP, led to an approximate 60% increase in torsional strength compared to girders without reinforcement. Furthermore, methods such as steel plate bonding and concrete jacketing were found to enhance torsional stiffness and strength by roughly 40% and 50%, respectively.

The inclusion of transverse reinforcement, such as closely spaced high-strength steel stirrups [18] or spiral reinforcement [19, 20], is critical for improving

the torsional behavior of reinforced concrete (RC) beams. This sort of reinforcement serves to contain the concrete, lowering the likelihood of shear crack development and boosting the beam's torsional strength. Other effective strategies include increasing the longitudinal reinforcement ratio [21] by integrating materials such as steel rebar. This technique increases the beam's torsional resistance by adding tensile strength throughout its length, hence improving its overall performance under torsional pressures.

Stepped concrete beams are pivotal in structural engineering as they effectively handle complex load distributions and adapt to various architectural needs. Commonly employed in multi-story buildings and structures with varying floor levels, such as staircases or ramps, these beams facilitate efficient load transfer between different heights. Their stepped design ensures both structural stability and flexibility, allowing them to support architectural features while maintaining load-bearing capacity across elevation changes. Moreover, stepped concrete beams enhance a building's aesthetic by seamlessly integrating structural elements into the overall design. Research has shown that CFRP composites can significantly boost the torsional strength of defected RC beams, achieving approximately a 70% performance increase, as noted by Afefy et al [22]. Additionally, the study by Fayed et al [23] demonstrated that altering beam configurations could enhance torsional capacity by up to 50%, illustrating the influence of reinforcement design on performance. Furthermore, Hamoda et al [24] found that beams with disturbed depths exhibited reduced torsional strength, but appropriate reinforcement could recover up to 40% of the lost capacity, highlighting the critical role of reinforcement strategies in preserving structural integrity.

This numerical study investigates the structural behavior of reinforced concrete stepped beams (RCSBs) with various reinforcement patterns. A numerical model was developed and validated against experimental data previously published by Eltaly et al. [17]. Following this, a numerical analysis was performed to assess different reinforcement techniques aimed at enhancing the torsional resistance of these beams. The first factor examined was stirrup spacing (SSs), with three beams constructed using varying stirrup spacings. The second factor was stirrup diameters (SDs), where two beams were tested with different stirrup diameters. The third factor involved the (LRR), with three beams featuring different longitudinal reinforcement levels. The fourth factor was (LRP), where three beams were designed with various reinforcement configurations in the drop zone. Key performance indicators, including bending angles at cracking and ultimate stages ($\theta cr$ and $\theta u$), bending moments at cracking (Mcr), maximum bending moments (Mu), (K), (E), and (D), were analyzed and compared to a baseline CS beam to identify improvements in the performance of the stepped beams.

## 2.The Considered Previous Experimental Study

Eltaly et al. [17] conducted a torsion behavior study on reinforced concrete box girders with openings, that have been strengthened, as shown in Figure 1. The study reveals that strengthening reinforced concrete box girders with fiber-reinforced polymers (FRP) significantly enhances torsional capacity, with improvements of up to 40% in strength and 30% in reduced deformation compared to non-strengthened girders. Openings in the girders decrease torsional strength by 20-25%, but FRP strengthening effectively mitigates this reduction, bringing performance closer to that of solid girders. The analytical models used to predict torsional behavior were validated with high accuracy, showing deviations within 10% of experimental results. The most effective strengthening configuration involved wrapping FRP around the entire girder perimeter. Larger and more poorly positioned openings had a greater negative impact on strength but strengthened improved load-carrying capacity by up to 35% and reduced distress and failure severity. Long-term performance of the strengthened girders remained robust, suggesting that FRP strengthening is a durable and effective solution for improving torsional performance in girders with openings, Eleven RC box girder specimens were evaluated under pure torsional conditions in the experimental study. All test specimens were constructed with constant dimensions and reinforcement. To evaluate the impact of various opening configurations and retrofitting techniques, carbon fiber reinforced polymer (CFRP) and steel plates were employed in different arrangements. Each box girder measured 1300 mm in length and had a square cross-section of 350 mm by 350 mm. The interior dimensions of each specimen were 200 mm by 200 mm. A single beam with identical external dimensions and length was also included. Longitudinal reinforcement consisted of eight 8 mm diameter bars. Transverse reinforcement was provided by closed stirrups with a 6 mm diameter, spaced 150 mm apart.

The mixture of concrete was created utilizing the ACI318-05 [1] method in order to get the concrete mix's contents, which reached a 50 N/mm2 strength. The mixing water ratio and Master Rh880 might be changed with the use of three mixers. as shown in Table 1. The cover's thickness for each tested specimen was 25 mm, as well as the reinforcing configurations and girder geometry were carefully considered above. There is one specimen as a solid beam CS, which is the under-study beam, with the same dimensions 1300 mm length and 1100 mm tested length with 8 mm diameter for 8 longitudinal bars and 6 mm diameter of stirrups with 150 mm spacing, shown in Figure 2. A 3000 kN hydraulic jack system was used to test the specimens in pure torsion, enabled by steel frame load arms on contrary sides. A concentrated load was applied on a rigid steel I-beam to distribute the load evenly. The supports allowed rotation of the three main axes while being vertically restrained at mid-width. The twist angle was calculated using the applied torque and LVDTs, with the average readings confirming the results as demonstrated in Figure 1.

Figure 1-Test setup and instrumentation

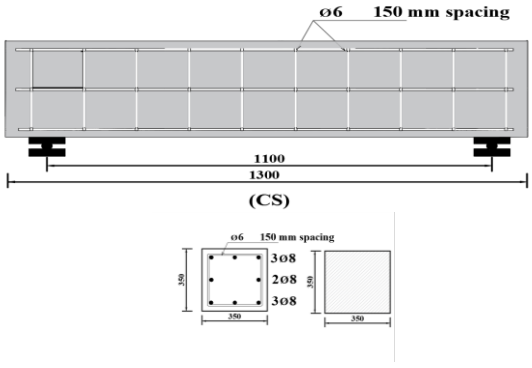


Figure 2-The under-study beam CS: Geometric and reinforcement properties (all dimension in millimeters)

**3.Preparation and Creation of Numerical Model.**

A three-dimensional Finite Element Model (FEM) for CS specimen, from reinforcement concrete box girders (RCBGs) test program, was developed using the ABAQUS software [25]. The first and second FEMs incorporated material properties and geometric parameters based on previously published experimental work on CS specimens conducted by Eltaly et al. [17]. The FEM results were validated by comparing them with the previous experimental data in terms of the torsional moment-angle of twist response, cracking, and failure modes. After successful validation, the model was used to perform a parametric study on the effectiveness of different reinforcement techniques for RCSBs, including variations in stirrup spacings (SSs) and stirrup diameters (SDs), (LRR), and (LRP).

**3.1.Constitutive Modeling of Materials and Sensitivity of Numerical Parameters**

To characterize the plastic mechanical behavior of concrete, the Concrete Damage Plasticity (CDP) model was selected. because it effectively simulates deterioration caused by nonlinear deformation and cracking under both tension and compression. This model is available in the ABAQUS software package, as illustrated in Figure 3. The material constitutive models for concrete material under tensile and compressive stresses are shown in Figure 4, respectively. Several Finite Element Models (FEMs) were carried out to assess sensitivity and identify the ideal constitutive parameters. for accurately describing the CDP model for concrete [26-28]. These parameters include dilation angle (ψ), viscosity relaxation parameter (μ), eccentricity (e), the ratio of biaxial to uniaxial compressive yield stresses (fbo/fco), and the ratio of the second stress invariant on the tensile to the compressive meridian (Kc). The Kc value ranged from 0.65 to 0.85, with the default value of 0.68 in ABAQUS yielding satisfactory results. The fbo/fco ratio ranged from 1.10 to 1.16, with a value of 1.16 providing acceptable validation, as noted by [29]. The eccentricity value used was the default of 0.1. Various viscosity parameters (0.00, 0.0002, 0.0004, 0.0006, 0.0008, and 0.001) were tested, with numerical results showing sensitivity to a zero value, as recommended by Eurocode [2]. The optimal dilation angle for both concrete was found to be 35, as recommended by [30], after testing angles ranging from 10 to 55. The Poisson's ratios for steel, and concrete were set at 0.3, and 0.2 respectively. Reinforcing steel bars and stirrups were modeled using a linear elastic-plastic model, as shown in Figure 4c.

Table 1 -Test findings for Mix's hardened concrete.

| Age | Compressive Strength kg/cm2 | | | | | | | | | | | Fcu kg/cm$^2$ |
|---|---|---|---|---|---|---|---|---|---|---|---|---|
| | 1 | 2 | 3 | 4 | 5 | 6 | 7 | 8 | 9 | 10 | 11 | |
| 7 | 337 | 342 | 338 | 345 | 378 | 374 | 381 | 344 | 358 | 371 | 369 | 358 |
| 28 | 538 | 544 | 535 | 552 | 587 | 563 | 592 | 547 | 551 | 560 | 558 | 557 |

The linear behavior represents the elastic stage up to the yield point, followed by a linear stage with hardening behavior fit for the ultimate load. Models were used for the steel bars: longitudinal steel bars with 8 mm diameter, and one with 10 mm diameter, also stirrups made of 6 mm diameter mild steel, and another two beams with 8 mm, and 10 mm diameter.

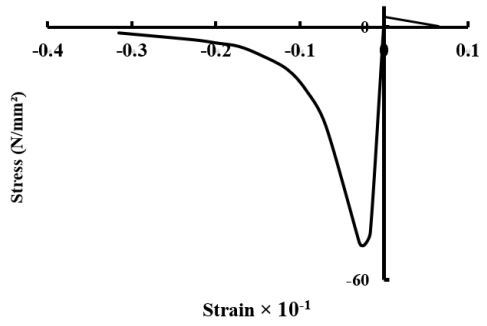


Figure 3-CDP model provided by ABAQUS.

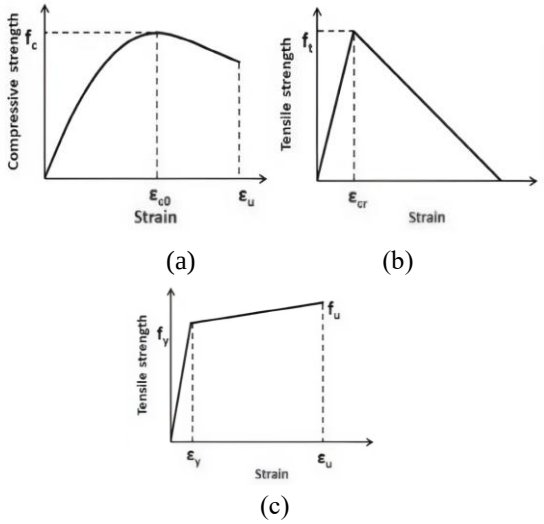


Figure 4-Materials constitutive models used in FEM for concrete [48]; (a) Concrete in compression, (b) Concrete in tension, and (c) Steel.

**3.2.Model Set-up**

The main components of the FEMs were concrete and steel bars. A model was developed and analyzed to validate the FEM used. The solid continuum formula was employed to model the beam CS, while wire elements were used for the steel bars. Three-dimensional, two-node truss elements (T3D2) in ABAQUS software was used to represent the steel bars and stirrups, while three-dimensional, eight-node linear hexahedral solid elements with reduced integration (C3D8R) were used to replicate the beam CS geometry. Figure 5(a) shows the model setup, while Figure 5(b) displays the arrangement of the reinforcing steel bars and stirrups. The Y direction was set to zero to represent the roller support. The beam could not translate in the X and Z directions because of the anti-symmetry boundary condition. Instead of applying an applied load, a vertical displacement in the Y direction was used to provide an accurate representation of the curves beyond the peak point. These boundary conditions are illustrated in Figure 5(a). Figures 6 shows views of the developed FEM for the beam CS. With the use of ABAQUS' embedded element constraint, it was expected that the type of concrete and the reinforcing steel bars/stirrups would interact perfectly. This constraint allowed the steel bars to be embedded in the concrete beam as a host region. The inner surface area of the RC CCBs was calculated to determine the total force acting on the beams during cracking and ultimate stages by multiplying the applied internal pressure stress by the area. the samples were subjected to loading rate with different final load values, and the total load for both stages was then calculated.

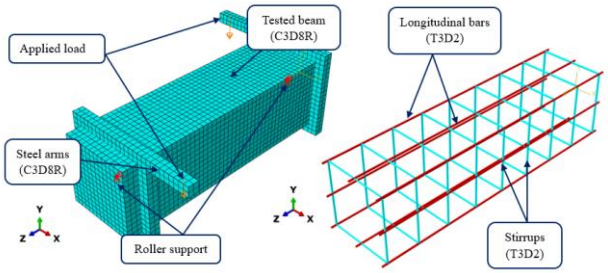


Figure 5-Model set-up: (a) Concrete elements type, loading, and boundary condition, and (b) Types of steel elements.

### 3.3.FEM Validation

The results from previous experimental studies by Eltaly et al. [17]. were compared with those from the FEMs in this section. The torsional moment-angle of twist response for the Beam CS are illustrated in Figure 6. For beam CS , the FEM results closely matched the experimental outcomes. The effect of the steel reinforcement ratio and geometric properties for CS was similar to the experimental results, demonstrating that the FEM could reasonably predict the behavior of CS in terms of torsional moment capacity, moment-twist curves, and failure modes. The numerical results and experimental data were compared and analyzed to verify the accuracy and validity of the established model, showing very similar outcomes. The proper representation of the samples, despite the different variables types used, contributed to these results. The crack patterns obtained from the FEM were compared to those from experimental observations and are shown in Figure 7. Initially, minor surface cracks and spalling indicate the onset of torsional stress. As the load increases, prominent diagonal cracks form, characteristic of torsional loading where shear stress results in helical crack patterns. These diagonal cracks extend across the beam, indicating significant torsional stress and deformation. The progression of these cracks, becoming wider and more pronounced, shows the beam approaching a critical failure stage. This pattern confirms the typical torsional failure mechanism in reinforced concrete beams, with diagonal cracks reflecting the shear stress paths within the structure. For the beam CS, initial cracks appeared on a place near to support with an inclined orientation at a total torsional moment of about 26.18 kN.m (experimental) and 27.94 kN.m (numerical), with a 6.72% variation in the cracking stage. With increased loading, crack widths expanded, and additional cracks appeared. The FEM peak torsional moment was 46.01 kN.m, compared to 43.87 kN.m experimentally, showing a 7.89% variation in peak moment. There was more validation in terms of yield and ultimate angle of twist . the yield twist was about 0.0038 radian /m (experimental) and 0.0041 radian /m (numerical), with a 5.4% variation. The ultimate twist for the first beam was about 0.0105 radian /m(experimental) and 0.0099 radian /m (numerical), with a 6.06 % variation. The FEM results showed a satisfactory correlation with the experimental results, with variations in both the elastic and plastic stages. This numerical model effectively simulates CS and its Geometric and reinforcement techniques. The same parameters will be used in a subsequent parametric study on the application of variations in stirrup spacings (SSs), stirrup diameters (SDs), (LRR), and (LRP). Also the interaction between the steel arm and the reinforced concrete beam was created using the merge instance function in the assembly module. The steel arms are modeled as elastic, while the reinforced concrete beam is modeled as a CPD material. The combined structure of the beam and arms is treated as a single unit, ensuring a strong connection despite their different material properties.

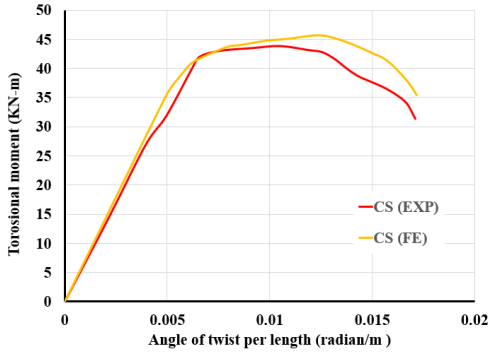


Figure 6- Torsional moment-twist relationships that obtained experimentally by published previous work [17] compared with (FE).

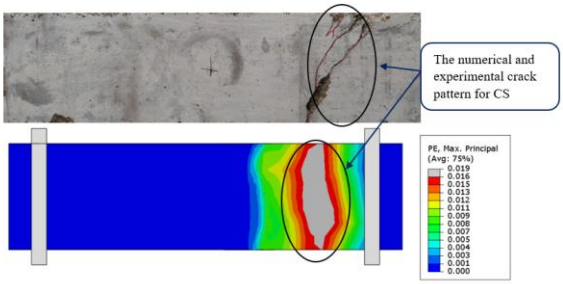


Figure 7 -Crack pattern and failure modes of CS.

**3.4.Parametric Study on Reinforcement patterns of (SSs), (SDs), (LRR), and (LRP).**

Newly, in reinforced concrete (RC) structures, uniformly depth RC beams have become usual. However, beams with varying depths can be geometrically advantageous for accommodating uneven floor slab systems and allowing utilities like pipes to pass through the beam depth without raising the floor height. These structures are frequently subjected to various stresses, making them essential to employ reinforcement methods that maintain their original dimensions and shape with high torsional capacity. By optimizing the distribution of reinforcement, stepped beams can effectively handle complex loading conditions and maintain their structural integrity. This study focuses on evaluating the behavior of RCSBs, aiming to capture the effect of (SSs), (SDs), (LRR), and (LRP) as a various parameters effect on the structural performance to resist the torsional loads. A comprehensive parametric analysis was performed using validated Finite Element Models (FEMs) to assess the impact of RCSBs application, including variations parameters. Ten RCSBs, organized into four groups, were numerically analyzed to failure. The parameters for each group are summarized in Table 2. Each beam was built with the same geometric characteristics and reinforcing features., as shown in Figure 8, with dimensions of 1300 mm length, 1100 mm test length, 350 x 350 mm cross-section dimensions. All tested beams have the same drop geometric properties, represented in 175 mm height and 175 mm width, as a ratio equal 0.50 from the beam depth, and the drop place is in the middle of the tested beam. The first group included three RCSBs which have the same longitudinal reinforcement, 8Ø8, and the reinforcement shape in the Drop zone is type 1(Figure 9) in the shapes of the longitudinal steel bars in the drop zone. In addition to the diameter of the stirrups used is 6 mm, but the difference between the sample of this group is in the distribution of the stirrups at different distances, which are 100 mm, 150 mm, and 200 mm for beams B1, B2, and B3, respectively. The second group consists of two RCSBs) and have the same characteristics in the distance of the stirrup's distribution, which is 150 mm, and the longitudinal steel used is 8Ø8, and its drop zone shape is type 1, as shown in Figure 9. Each of them differs in the diameter of the stirrups used, which are 8 mm diameter and 10 mm diameter for beams B4 and B5, respectively. The third group consists of three RCSBs beams, and the stirrup diameter is 6 mm, the distance between the stirrups is 150 mm, and the reinforcement shape is type 1 as shown in Figure 9. But the difference lies in changing the ratio of longitudinal steel to the cross-section of the beam as ratios of 0.246% (6Ø8), 0.411% (10Ø8), and 0.513% (8Ø10) for beams B6, B7, and B8, respectively, knowing that the reinforcement ratio of beam B2, which is constant in the remaining beams, represents 0.328% (8Ø8), which is the beam being compared with that group. The fourth group included two RCSBs. The change in it came in the form of the longitudinal steel connection in the drop zone. The two beams were types 2 and 3 for beams B9 and B10, respectively, as shown in Figure 9, with the previous parameters remaining constant for these beams. The FEM of CS sample, which was derived from the experimental verification, was used as a control beam for the rest of the groups and compared with it, as it has a stirrups distribution distance of 150 mm and 8Ø8 longitudinal steel is used as shown in Figure 8(a). The main objective of this study is to compare the enhancements due to reinforcement changing in terms of cracking and ultimate stages, (K), (D), and (E). All strengthened RCSBs were analyzed using the same validated FEM as shown in Figure 10. The details of the FEMs used in this parametric study, including loading, interactions, boundary conditions, and element types, are outlined in this section. Concrete for concrete was modeled using continuum, three-dimensional, eight-node linear hexahedral solid elements with reduced integration (C3D8R) in ABAQUS. The reinforcement steel bars, and closed stirrups were represented using two-node linear truss elements (T3D2). The boundary conditions included loading and supporting systems, with models supported on 3D roller supports. Loads were applied as a vertical displacement gradually loaded. The interaction between steel bars/stirrups and concrete was simulated using tie interaction, When the truss elements, which represented the reinforcing bars/stirrups, were the embedded region and the concrete beam acted as the host region. This modeling was consistent with the basic model in this study after validation. The same test setup was applied to all 10 FEMs. The groups were studied to evaluate the most effective reinforcement for increasing RCSBs torsional moment capacity and improving overall structural behavior. The beams RCSBs details are illustrated in Figure 10(b, c, d, and e) for groups G1, G2, G3, and G4, respectively.

Table 2-Test matrix

| Group | Specimen`s ID | Stirrups Spacing "mm" | Stirrup Diameter "mm" | Longitudinal Reinforcement Ratio "%" | Longitudinal Reinforcement Patterns | Studied parameter |
|---|---|---|---|---|---|---|
| G1 | B0=CS | 150 | Ø6 | 0.328 % (8Ø8) | ——— | SSs |
| | B1 | 100 | | | Type (1) | |
| | B2 | 150 | | | | |
| | B3 | 200 | | | | |
| G2 | B0=CS | 150 | Ø6 | 0.328 % (8Ø8) | ——— | SDs |
| | B2 | | Ø6 | | Type (1) | |
| | B4 | | Ø8 | | | |
| | B5 | | Ø10 | | | |
| G3 | B0=CS | 150 | Ø6 | 0.328 % (8Ø8) | ——— | LRR |
| | B2 | | | 0.328 % (8Ø8) | Type (1) | |
| | B6 | | | 0.246 % (6Ø8) | | |
| | B7 | | | 0.411 % (10Ø8) | | |
| | B8 | | | 0.513 % (8Ø10) | | |
| G4 | B0=CS | 150 | Ø6 | 0.328 % (8Ø8) | ——— | LRP |
| | B2 | | | | Type (1) | |
| | B9 | | | | Type (2) | |
| | B10 | | | | Type (3) | |

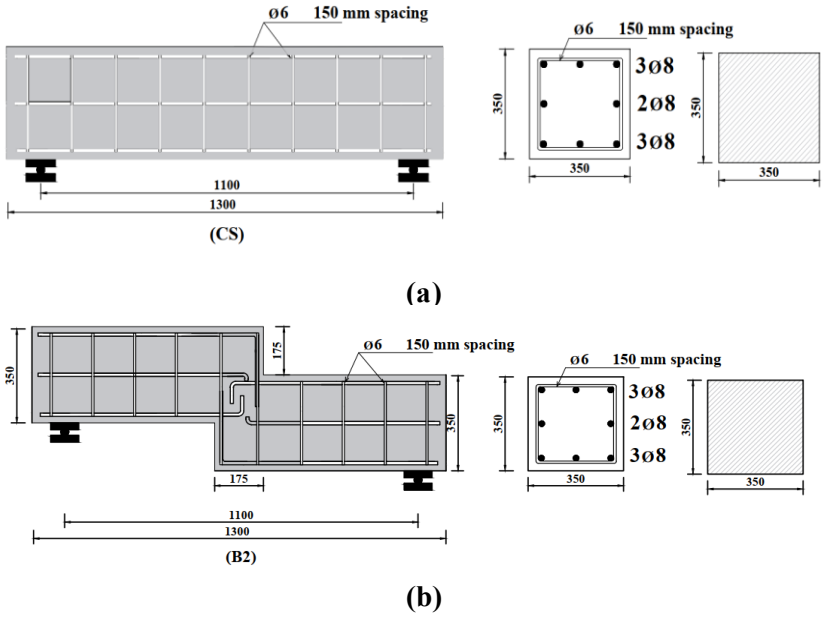


Figure 8-Geometric and reinforcement details for: (a) beam CS, (b) beam B2.

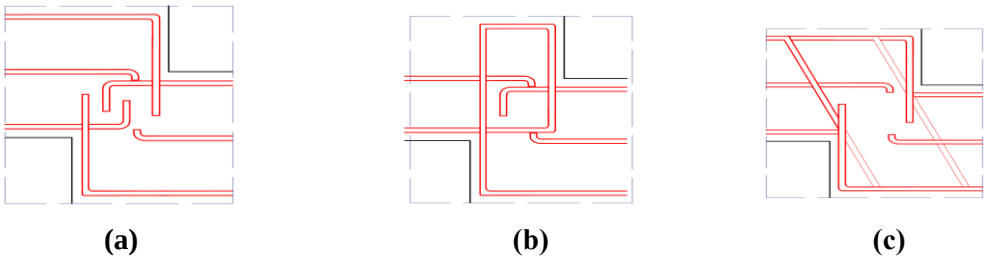


Figure 9-Longitudinal reinforcement patterns: (a) type (1), (b) type (2), and (c) type (3).

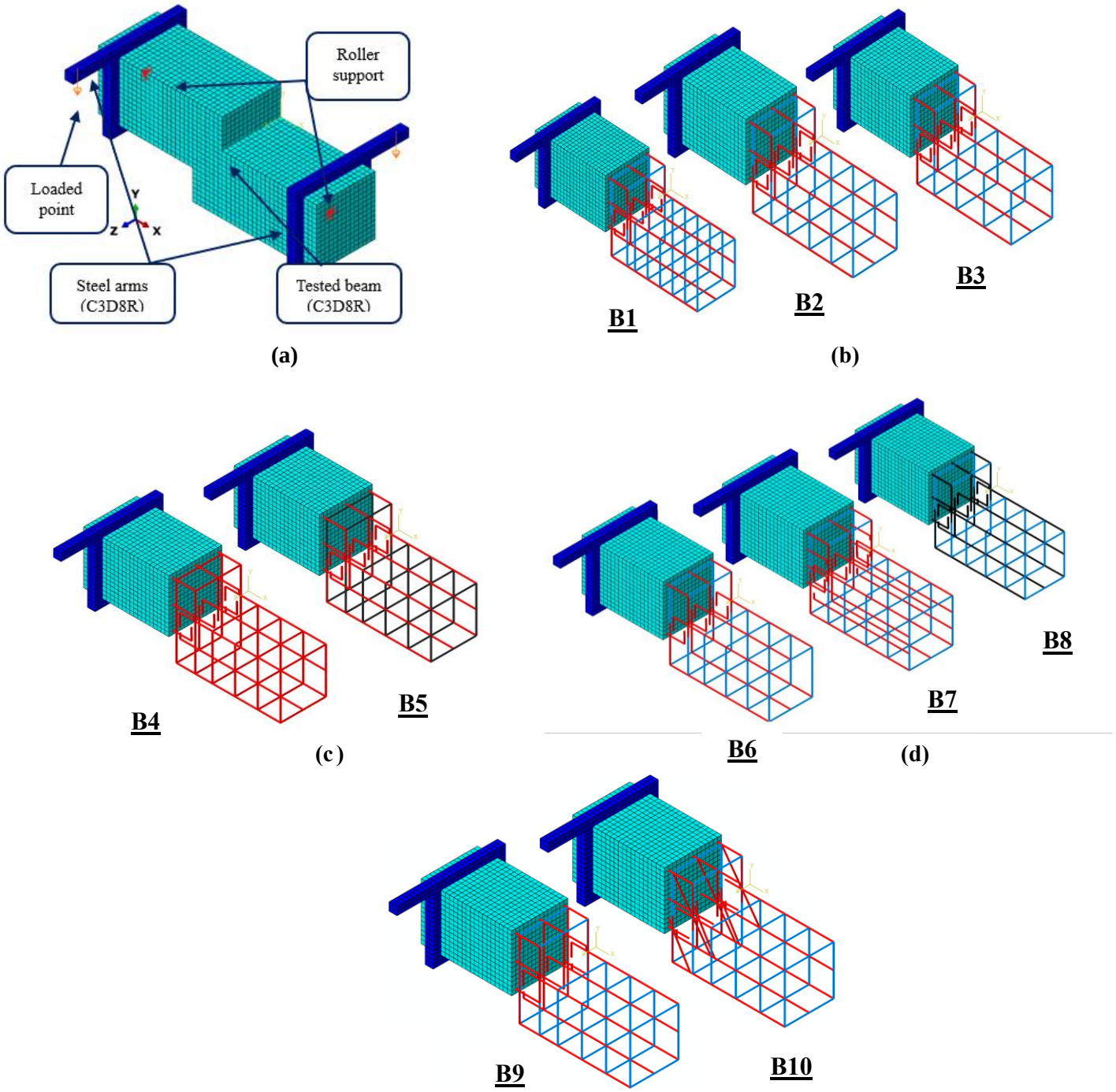


Figure 10-Model set-up for all groups: (a) Types of elements, loading, and boundary condition, (b) Group G1, (c) Group G2, (d) Group G3, and (e) Group G4.

**3.4.1.Effect of Application of (SSs)**

The values of the relevant torsional angles of the ultimate and cracking phases (θcr) and (θu) are displayed in Table 3. (, respectively as an impression of the linear width and the same values but in torsional moment (Mcr) and (Mu). The numerical moment-torsion curves of the studied beams are depicted in Figure 12(a, b, c, d) for groups G1, G2, G3 and G4, respectively. One of the main objectives of this parametric study is to capture the influence of SSs on the torsional behavior of reinforced concrete RCSBs. The effect of three different for SSs is investigated in this section. Three specimens with the same RCSBs geometrical details and reinforcement are considered to evaluate the influence of SSs and their arrangement on their torsional resistance. For beams B1, B2, and B3, the corresponding spacings were 100 mm, 150 mm, and 200 mm. The results of these FEMs were compared with a main beam (B0) to investigate the effect of SSs on stepped beams. The numerical results of the FEMs for the three beams are shown Table 3. The elastic stiffness index (K) and (E) were chosen for comparison for all reinforced beams as a clear indicator for comparison and to determine the behavior of reinforced concrete beams in addition to knowing the value of (D) to know the ability of beams to create a larger torsion angle which is reflected in their ability in the maximum torsional moment. It was found that the new application of SSs led to an improvement in E by about 0.32-0.63 than the estimated from the main beam B0. The estimated K was presented as a slope of the linear curve in Table 3. It was found that the application of SSs led to an improvement in K by about 0.87-0.91 than the estimated from the main beam B0. There was also an improvement in (D) by about 0.72-0.83. In fact, the presence of SSs enhanced the performance of torsion angle, crack loads, ultimate loads, (K), (E)and (D) to moderate values where the average values (AVG) of these values ranged from 0.92-0.62. The crack pattern in the studied numerical SSs was around the distribution of the kerfs where these stresses and cracks are shown in Figure 13(a). The cracks are at 45° angle with medium number of cracks and somewhat circular regular patterns around the stirrups under shear stresses.

**3.4.2.Effect of Application of (SDs)**

The effect of SDs on the torsional behavior of reinforced concrete RCSBs was of great importance. Different beams in SDs were divided into two beams B4 with 8 mm diameter and B5 with a 10 mm diameter. The results of these FEMs were compared with a main beam (B0) to investigate the effect of SDs on the listed beams. The numerical results of FEMs for the two beams are shown in Table 3. It was found that the new application of SDs resulted in an improvement in E of about (0.53-0.77) over the estimated one from the main beam B0. It was found that the application of SDs resulted in an improvement in (K) of about (0.90-0.94) over the estimated one from the main beam B0. There was also an improvement in (D) of about (0.82-0.89). In fact, the presence of SDs enhanced the performance of torsion angle, crack loads, ultimate loads, (K), (E), and (D) to superior values where the average values (AVG) of these values ranged from (0.75-0.94) with a standard deviation (SD) ranging from (0.04-0.20) in addition to a high coefficient of variation ranging from (0.04-0.27) as shown in Table 3, a value that shows the superiority of this group over the rest of the groups, which illustrates the significant effect of the stirrup diameter on torsional resistance. The crack pattern in the numerical SDs studied was around the crack distribution where these stresses and cracks are shown in Figure 13(b). 45-degree cracks with a large number of cracks and irregular patterns due to spalling under shear stresses and additional spalling stresses.

**3.4.3.Effect of Application of (LRR)**

The impact of (LRR) on the torsional behavior of reinforced concrete stepped beams (RCSBs) was significant. The beams were categorized into three beams: B6, B7, and B8, with longitudinal reinforcement ratios to the cross-sectional area of concrete of 0.246% (6Ø8), 0.411% (10Ø8), and 0.513% (8Ø10) respectively. These FEM results were compared to the main beam (B0) to examine LRR's effect. Table 3 shows the numerical results for the beams. The application of LRR improved (E) by about 0.53-0.90 times compared to the main beam B0. (K) was improved by about 0.84-0.97 times. (D) also saw an enhancement of about 0.68-0.93 times. LRR enhanced the torsion angle performance, crack loads, ultimate loads, (K), (E), and (D) to high values, with average (AVG) values ranging from 0.70-0.93 and a standard deviation (SD) from 0.06-0.31, along with a coefficient of variation (CoV) from 0.06-0.44, as shown in Table 3. This group ranked second in performance after Group G2. Although beams B8 and B7 exhibited high torsional resistance, beam B6 showed the lowest, resulting in that overall ranking. The crack patterns in the numerical LRR study, shown in Figure 13(c), featured 45-degree cracks with moderate frequency and fairly regular patterns along the longitudinal reinforcement under longitudinal stresses.

**3.4.4.Effect of Application of (LRP)**

The impact of the (LRP) on the torsional behavior of reinforced concrete stepped beams (RCSBs) was the least significant factor. The beams were categorized into two types: B9 and B10, with reinforcement configurations in the landing zone corresponding to cross-sectional areas of type 2 and type 3, as illustrated in Figure 10. These FEM results were compared to the main beam (B0) to assess the effect of LRP. Table 3 presents the numerical results for the beams. LRP improved the performance of torsional angle, crack loads, ultimate loads, (K), (E), and (D) to high levels, with mean values (AVG) ranging from 0.58-0.91, a standard deviation (SD) from 0.06-0.29, and a coefficient of variation (CoV) from 0.07-0.50, as shown in Table 3. This group ranked last in torsional strength due to the relatively low torsional strength of B9 and B10, and the reinforcement shape in the landing zone not sufficiently enhancing the stepped beams' torsional strength. The crack patterns in the LRP numerical study, depicted in Figure 13(d), exhibited 45° cracks with a moderate number of irregularly spaced cracks under shear stress.

**3.4.5.Ultimate torsional moment**

The resistance of the 11 beams to the maximum torsional moments is shown in Figure 11, where beam B0 came in the lead with the highest value of 45.57 kN.m, which is a structural behavior similar to that studied in [23] and it shows the advantage of straight beams over stepped beams. Then came beams B8 and B7 with maximum torsional moments of 44.21 and 43.29 kN.m, respectively, which showed the importance of longitudinal reinforcement in the case of these beams, as is consistent with the structural behavior in [21].In contrast, B6 reached one of the torsional moments 26.43 kN.m because it has the lowest longitudinal reinforcement ratio. As for the following beams, were diameter of the beams in beams B5 and B4 was 41.47 and 36.65 kN.m respectively, which reinforces the idea of changing the diameter of the beams and their importance in resisting torsion. Then came the distribution of the passengers, represented by beams B1 and B2, with values of 37.83 and 35.55 kN.m respectively, which indicates the importance of the distances of the passengers' distribution on resisting the torsion capacity, which is consistent with the behavior of the thresholds in [20], while B3, which is in the same group, comes in the penultimate place with a maximum torsional moment of 29.17 kN.m due to increasing the distribution distance between the stirrups to 200 mm, which weakens the beam's resistance to torsion. In a lower range are beams B10 and B9 with maximum torsional moment values of 33.73 and 30.99 kN.m, which indicates that the effect of the shape of the longitudinal reinforcement in the drop zone does not significantly affect the torsional resistance, as is clear in the behavior of [20]. Figure 11 shows the difference between different values of torsional moments for the RCSBs and the straight beam B0.

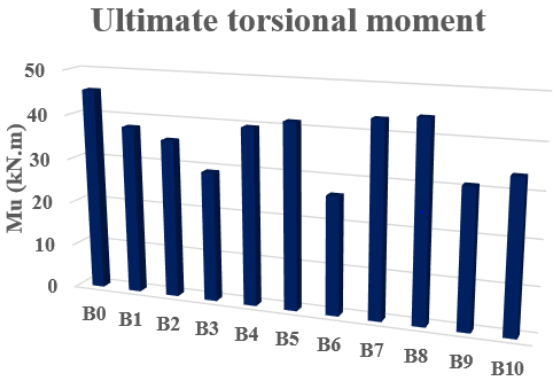


Figure 11- Ultimate moment for tested beam obtained Numerically .

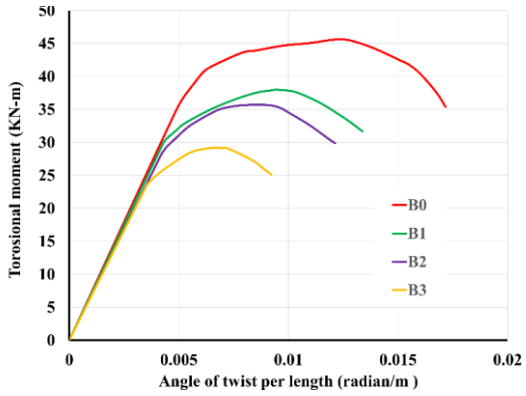


**(a)**

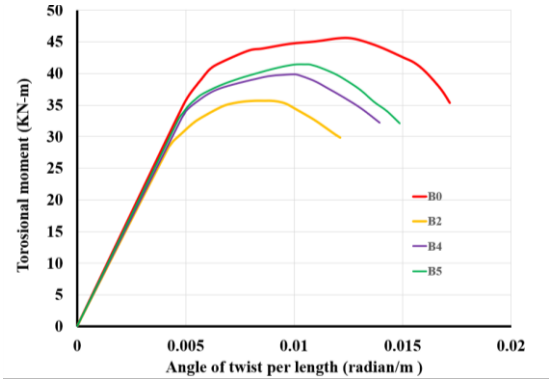


**(b)**

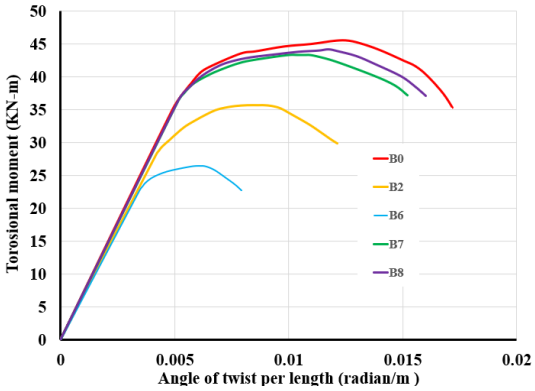


**(c)**

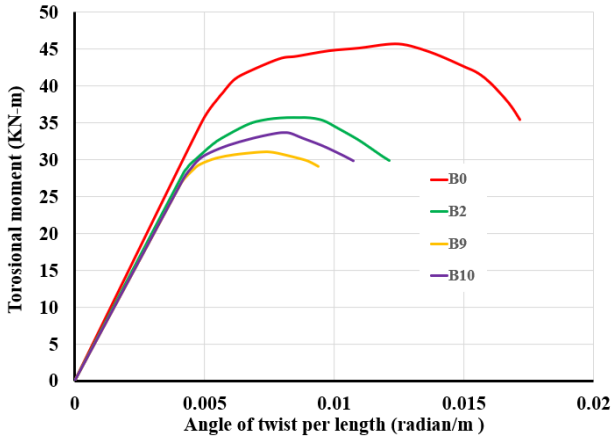


**(d)**

Figure 12-Moment-twist relationships obtained Numerically: (a) Group G1, (b) Group G2, (c) Group G3, and (e) Group G

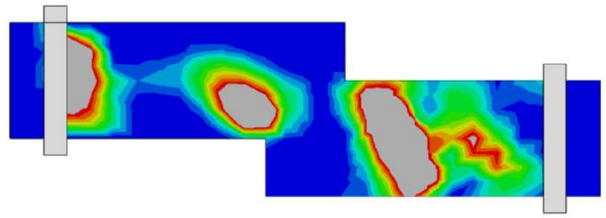

**(a)**

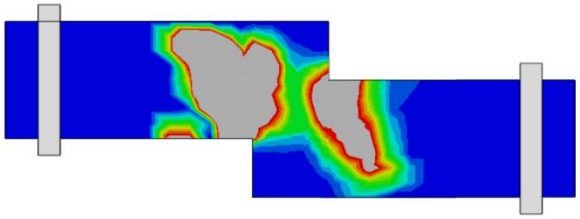

**(b)**

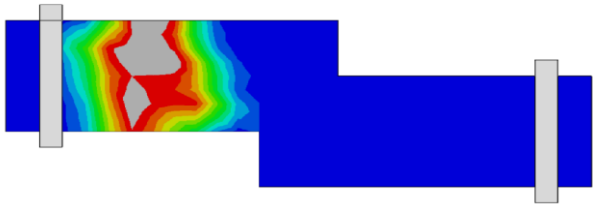

**(c)**

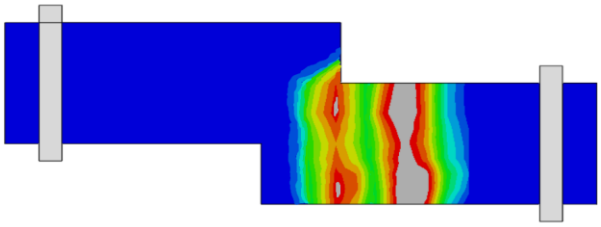

**(d)**

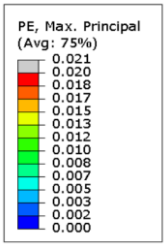


Figure 13-Crack pattern of numerical results: (a) B2 of SSs group, (b) B4 of SDs group, (C) B7 of LRR group, and (d) B9 of LRP group.**PE, Max. principal:** maximum principal plastic strain energy

Table 1-Numerical results.

| Group | Specimen ID | Cracking Stage | | | Ultimate Stage | | | Elastic Stiffness index ( K) | K / $K_{B0}$ | Ductility index ( D) | D / $D_{B0}$ | Absorbed Energy ( E ) | E / $E_{B0}$ |
|---|---|---|---|---|---|---|---|---|---|---|---|---|---|
| | | $M_{cr}$ (kN.m) | $M_{crB}$ / $M_{crB0}$ | $\theta_{cr}$ (radian/m) | $M_u$ (kN.m) | $M_u$/ $M_{u\,B0}$ | $\theta_u$ (radian/m) | | | | | | |
| G1 | B0 | 36.67 | 1 | 0.0049 | 45.57 | 1 | 0.01264 | 7483.88 | 1 | 2.58 | 1 | 0.6103 | 1 |
| | B1 | 29.83 | 0.81 | 0.00437 | 37.83 | 0.83 | 0.00948 | 6826.09 | 0.91 | 2.15 | 0.83 | 0.3857 | 0.63 |
| | B2 | 28.24 | 0.77 | 0.0042 | 35.55 | 0.78 | 0.00885 | 6723.81 | 0.9 | 2.11 | 0.82 | 0.3252 | 0.53 |
| | B3 | 23.38 | 0.64 | 0.0036 | 29.17 | 0.64 | 0.00695 | 6476.18 | 0.87 | 1.87 | 0.72 | 0.1979 | 0.32 |
| | AVG | | 0.81 | | | 0.81 | | | 0.92 | | 0.84 | | 0.62 |
| | SD | | 0.15 | | | 0.15 | | | 0.06 | | 0.12 | | 0.28 |
| | CoV | | 0.19 | | | 0.19 | | | 0.07 | | 0.14 | | 0.45 |
| G2 | B0 | 36.67 | 1 | 0.0049 | 45.58 | 1 | 0.01264 | 7483.88 | 1 | 2.58 | 1 | 0.6103 | 1 |
| | B2 | 28.24 | 0.77 | 0.0042 | 35.55 | 0.78 | 0.00885 | 6723.81 | 0.9 | 2.11 | 0.82 | 0.3252 | 0.53 |
| | B4 | 32.77 | 0.89 | 0.0047 | 39.65 | 0.87 | 0.01011 | 6957.54 | 0.93 | 2.17 | 0.84 | 0.4197 | 0.69 |
| | B5 | 32.87 | 0.9 | 0.0046 | 41.47 | 0.91 | 0.01074 | 7022.86 | 0.94 | 2.3 | 0.89 | 0.467 | 0.77 |
| | AVG | | 0.89 | | | 0.89 | | | 0.94 | | 0.89 | | 0.75 |
| | SD | | 0.09 | | | 0.09 | | | 0.04 | | 0.08 | | 0.2 |
| | CoV | | 0.1 | | | 0.1 | | | 0.04 | | 0.09 | | 0.27 |
| G3 | B0 | 36.67 | 1 | 0.0049 | 45.58 | 1 | 0.01264 | 7483.88 | 1 | 2.58 | 1 | 0.6103 | 1 |
| | B2 | 28.24 | 0.77 | 0.0042 | 35.55 | 0.78 | 0.00885 | 6723.81 | 0.9 | 2.11 | 0.82 | 0.3252 | 0.53 |
| | B6 | 22.71 | 0.62 | 0.0036 | 26.43 | 0.58 | 0.00632 | 6273.48 | 0.84 | 1.75 | 0.68 | 0.1523 | 0.25 |
| | B7 | 35.07 | 0.96 | 0.0048 | 43.29 | 0.95 | 0.01137 | 7215.23 | 0.96 | 2.34 | 0.91 | 0.5088 | 0`.83 |
| | B8 | 36.41 | 0.99 | 0.0050 | 44.21 | 0.97 | 0.01201 | 7266.67 | 0.97 | 2.4 | 0.93 | 0.5496 | 0.9 |
| | AVG | | 0.87 | | | 0.86 | | | 0.93 | | 0.87 | | 0.7 |
| | SD | | 0.17 | | | 0.18 | | | 0.06 | | 0.12 | | 0.31 |
| | CoV | | 0.2 | | | 0.21 | | | 0.06 | | 0.14 | | 0.44 |
| G4 | B0 | 35.07 | 0.96 | 0.0049 | 45.58 | 1 | 0.01264 | 7483.88 | 1.0 | 2.58 | 1 | 0.6103 | 1 |
| | B2 | 28.24 | 0.77 | 0.0042 | 35.55 | 0.78 | 0.00885 | 6723.81 | 0.9 | 2.11 | 0.82 | 0.3252 | 0.53 |
| | B9 | 26.44 | 0.72 | 0.0041 | 30.99 | 0.68 | 0.00758 | 6528.4 | 0.87 | 1.93 | 0.75 | 0.2142 | 0.35 |
| | B10 | 27.37 | 0.75 | 0.0042 | 33.73 | 0.74 | 0.00821 | 6532.22 | 0.87 | 1.96 | 0.76 | 0.2653 | 0.43 |
| | AVG | | 0.81 | | | 0.8 | | | 0.91 | | 0.83 | | 0.58 |
| | SD | | 0.13 | | | 0.14 | | | 0.06 | | 0.12 | | 0.29 |
| | CoV | | 0.16 | | | 0.18 | | | 0.07 | | 0.14 | | 0.5 |

**Mcr**: Torsional moment at which the first crack appeared; **θcr**: angle of twist recorded at Mcr; Mu: Ultimate torsional moment ; **θu**: Angle of twist at ultimate torsional moment ; **K**: Elastic index(kN.m/radian/m); ; **D**: Ductility index (unitless) **E**: Absorbed energy(kN.m.radian/m).

**4.Conclusions**

This study presents the numerical simulation and analysis of (RCSBs) featuring different properties. The beams, subjected to pure torsional loads, were analyzed using finite element models (FEMs). The accuracy of the FEM was previously validated by selecting (CS beam) that had been experimentally tested in a prior study[17], and then comparing the FEM results with those obtained from the experimental work. The findings demonstrate that FEM is effective in simulating RCBGs. Additionally, A parametric study was carried out to look at the impact of stirrup spacings (SSs), stirrup diameters (SDs), longitudinal reinforcement ratio (LRR), and longitudinal reinforcement patterns (LRP) on the structural performance of the modeled beams under applied loads. The main observations of this research are summarized as follows:

1- Straight beams offer higher torsional capacities, energy absorption, and stiffness than stepped beams, indicating better structural performance under torsional stresses.

2- The longitudinal reinforcement ratio has a direct effect on the beam's torsional capability. Torsional capacity improves overall as (LRR) increases. Torsional capacity has decreased by around 3% to 5%. In addition, (K), (D), and (E) values are reduced by 3-4%, 7-9%, and 10-17%, respectively, as compared to the straight beam B0. However, this results in a large increase in torsional capacity for the stepped beam B2, with a 22-24% improvement and equivalent improvements in (K), (D), and (E) of 7-8%, 11-14%, and 56-69%, respectively, over beam B2.

3- The performance of stepped beams is significantly impacted by the size of the stirrup diameters (SDs). Results have a reduction in torsional capacity, ranging from 9% to 13% when compared to the straight beam B0. However, in comparison to beam B2, the larger (SDs) lead to an 11-17% increase in torsional capacity, along with improvements of 3-4% in (K), 3-9% in (D), and 29-44% in (E).

4- The torsional capacity of the beam tends to drop as the stirrup spacing (SSs) increases, with a reduction in torsional capacity ranging from 17% to 36% compared to the straight beam B0. However, reducing the SSs results in a 6% increase in torsional capacity, accompanied by improvements of 2% in (K), 2% in (D), and 19% in (E), when compared to beam B2.

5- Changing the longitudinal reinforcement pattern (LRP) in the drop zone led to a significant reduction in torsional capacity, ranging from 26% to 32% compared to the straight beam B0. In comparison to beam B2, there is a decrease of 5-13% in (Mu), 3% in (K), 7-9% in (D), and 18-34% in (E).

**5.References**

[1] Committee A. Building code requirements for structural concrete (ACI 318-05) and commentary (ACI 318R-05). American Concrete Institute; 2005.

[2] Code P. Eurocode 2: design of concrete structures-part 1–1: general rules and rules for buildings. British Standard Institution, London. 2005;668:659-68.

[3] Uomoto T, Ishibashi T, Nobuta Y, Satoh T, Kawano H, Takewaka K et al. Standard Specifications for Concrete Structures-2007 by Japan Society of Civil Engineers. Concrete Journal. 2008;46:3-14.

[4] Park R, Paulay T. Reinforced concrete structures: John Wiley & Sons; 1991.

[5] Belarbi A, Prakash S, You Y-M. Effect of spiral reinforcement on flexural-sheartorsional seismic behavior of reinforced concrete circular bridge columns. Struct Eng Mech. 2009;33:137-58.

[6] Prakash S, Belarbi A, You Y-M. Seismic performance of circular RC columns subjected to axial force, bending, and torsion with low and moderate shear. Engineering Structures. 2010;32:46-59.

[7] Patel PV, Jariwala VH, Purohit SP. Torsional strengthening of RC beams using GFRP composites. Journal of The Institution of Engineers (India): Series A. 2016;97:313-22.

[8] Hadhood A, Gouda MG, Agamy MH, Mohamed HM, Sherif A. Torsion in concrete beams reinforced with GFRP spirals. Engineering Structures. 2020;206:110174.

[9] Zhou J, Shen W, Wang S. Experimental study on torsional behavior of FRC and ECC beams reinforced with GFRP bars. Construction and Building Materials. 2017;152:74-81.

[10] Safan M. Strength of short square columns confined with GFRP wraps. ERJ Engineering Research Journal. 2004;27:83-90.

[11] Saafan M. Shear strengthening of reinforced concrete beams using GFRP wraps. Acta Polytechnica. 2006;46.

[12] Al-Rousan R, Abo-Msamh I. Bending and torsion behaviour of CFRP strengthened RC beams. Magazine of Civil Engineering. 2019:48-62.

[13] Majeed AA, Allawi AA, Chai KH, Badaruzzam HW. Behavior of CFRP strengthened RC multicell box girders under torsion. Structural Engineering and Mechanics. 2017;61:397-406.

[14] Tibhe SB, Rathi VR. Comparative experimental study on torsional behavior of RC beam using CFRP and GFRP fabric wrapping. Procedia Technology. 2016;24:140-7.

[15] Yang S, Cao S, Gu R. New technique for strengthening reinforced concrete beams with composite bonding steel plates. Steel Compos Struct. 2015;19:735-57.

[16] Fawzy K, Farouk MA. Torsion strengthening of RC beams with external lateral pressure using steel plates. Iranian Journal of Science and Technology, Transactions of Civil Engineering. 2021;45:1413-25.

[17] Eltaly B, EL_Sayed M, Meleka N, Kandil K. Torsion behavior of strengthened reinforced concrete box girders with openings: Analytical and experimental investigation. Structures: Elsevier; 2024. p. 105908.

[18] Kim C, Kim S, Kim K-H, Shin D, Haroon M, Lee J-Y. Torsional Behavior of Reinforced Concrete Beams with High-Strength Steel Bars. ACI Structural Journal. 2019;116.

[19] Shatarat N, Katkhuda H, Alqam M. Experimental investigation of reinforced concrete beams with spiral reinforcement in shear. Construction and Building Materials. 2016;125:585-94.

[20] Chalioris CE, Karayannis CG. Experimental investigation of RC beams with rectangular spiral reinforcement in torsion. Engineering structures. 2013;56:286-97.

[21] Chiu H-J, Fang I-K, Young W-T, Shiau J-K. Behavior of reinforced concrete beams with minimum torsional reinforcement. Engineering Structures. 2007;29:2193-205.

[22] Afefy HME-D, Mahmoud MH, Fawzy TM. Rehabilitation of defected RC stepped beams using CFRP. Engineering structures. 2013;49:295-305.

[23] Fayed S, Basha A, Elsamak G. Behavior of RC stepped beams with different configurations: An experimental and numerical study. Structural concrete. 2020;21:2601-27.

[24] Hamoda A, Basha A, Fayed S, Sennah K. Experimental and numerical assessment of reinforced concrete beams with disturbed depth. International Journal of Concrete Structures and Materials. 2019;13:1-28.

[25] Hibbitt K, Sorensen. ABAQUS Theory Manual: Hibbitt, Karlsson & Sorensen; 1995.

[26] Hamoda AA, Eltaly BA, Sera RE, Liang QQ. Behavior of reinforced concrete stair slabs strengthened with steel plates and near surface mounted steel bars. Engineering Structures. 2023;292:116514.

[27] Hamoda A, Elsamak G, Emara M, Ahmed M, Liang QQ. Experimental and numerical studies of reinforced concrete beam-to-steel column composite joints subjected to torsional moment. Engineering Structures. 2023;275:115219.

[28] Hamoda AA, Eltaly BA, Ghalla M, Liang QQ. Behavior of reinforced concrete ring beams strengthened with sustainable materials. Engineering Structures. 2023;290:116374.

[29] El-Mandouh MA, Elsamak G, O. Rageh B, Hamoda A, Abdelazeem F. Experimental and numerical investigation of one-way reinforced concrete slabs using various strengthening systems. Case Studies in Construction Materials. 2023;18:e01691.

[30] Eltaly BA, Shaheen YB, Salem M, Hamoda A. Ferrocement oil pipes exposed to critical conditions and using various types of reinforcement mesh: Experimental and numerical studies. Structures. 2024;66:106780.